Effects of precompensation and postcompensation on timing jitter in dispersion-managed systems

J. Santhanam

Department of Physics and Astronomy, University of Rochester, Rochester, New York 14627

C. J. McKinstrie

Department of Mechanical Engineering, University of Rochester, Rochester, New York 14627

T. I. Lakoba and Govind P. Agrawal

Institute of Optics, University of Rochester, Rochester, New York 14627

Received March 1, 2001

We present an analytic theory of timing jitter in dispersion-managed light-wave systems that is based on the moment method and the assumption of a chirped Gaussian pulse. We apply the theory to a soliton system and show that 50% postcompensation of the accumulated dispersion can reduce the jitter by a factor of 2. We also apply the theory to a low-power light-wave system employing the return-to-zero format and find that timing jitter can be minimized along the fiber link for an optimal choice of precompensation and postcompensation.

OCIS codes: 060.5530, 060.2330, 060.4510, 190.5530.

Gordon–Haus timing jitter is known to impose a fundamental limitation on periodically amplified light-wave systems.[1,2] Recently, it was recognized that timing jitter can occur with any transmission format, including the nonreturn-to-zero, chirped-return-to-zero (CRZ), and dispersion-managed (DM) soliton formats,[3] and timing jitter can be calculated with the moment method.[4] In this Letter we present a simplified form of the moment method and show that it can provide approximate analytic expressions for the timing jitter as long as each bit in the DM system can be approximated by a chirped Gaussian pulse. We apply this technique to study the effects of precompensation and postcompensation on timing jitter in DM light-wave systems for both low-power CRZ and DM-soliton formats. We find that we can reduce timing jitter significantly by choosing the precompensation and postcompensation of residual dispersion judiciously.

Optical pulse propagation inside periodically amplified fiber links is governed by the nonlinear Schrödinger equation[2]:

$$i\,\frac{\partial A}{\partial z} - \frac{\beta_2}{2}\,\frac{\partial^2 A}{\partial t^2} + \gamma|A|^2 A = \frac{i}{2}\,g(z)A\,, \qquad (1)$$

where A represents the pulse envelope, β_2 is the group-velocity dispersion (GVD) coefficient, and γ is the nonlinear parameter. A typical DM system consists of a precompensation fiber, followed by a periodic sequence of anomalous and normal fibers and a postcompensation fiber. Fiber losses and periodic amplification are included in Eq. (1) through $g(z)$ such that $g(z) = -\alpha$ everywhere except at the location of lumped amplifiers. The parameters α, β_2, and γ are different for the anomalous- and normal-GVD fibers used to form the dispersion map. Although the nonlinear Schrödinger equation can be solved numerically, calculation of the timing jitter is time consuming because of the statistical nature of the problem.

In the moment method,[4] the temporal and frequency shifts of an optical pulse are calculated with

$$T(z) = \frac{1}{E}\int_{-\infty}^{\infty} t|A(z,t)|^2 \mathrm{d}t, \qquad (2a)$$

$$W(z) = \frac{i}{2E}\int_{-\infty}^{\infty} (A^* A_t - A A_t^*)\mathrm{d}t\,, \qquad (2b)$$

where A_t stands for the time derivative. The pulse energy, $E(z) = \int_{-\infty}^{\infty} |A(z,t)|^2 \mathrm{d}t$, itself varies along the link in a periodic fashion because of periodic compensation of fiber losses through amplifiers. Using the nonlinear Schrödinger equation and adding the random shifts occurring at each amplifier, we find that the frequency W and the temporal position T of the pulse evolve as

$$\frac{\mathrm{d}W}{\mathrm{d}z} = \sum_{j=1}^{N} \delta W_j \delta(z - z_j)\,, \qquad (3a)$$

$$\frac{\mathrm{d}T}{\mathrm{d}z} = \beta_2 W + \sum_{j=1}^{N} \delta T_j \delta(z - z_j)\,, \qquad (3b)$$

where δW_j and δT_j are the random frequency and time shifts imposed on the pulse at the jth amplifier located at z_j and N is the total number of amplifiers used within the DM system.

Further analysis requires the selection of a specific pulse shape. An exact calculation of timing jitter should use the numerical solution of Eq. (1), as discussed in Ref. 3. We use the Gaussian-shaped ansatz that is commonly used for variational analysis of DM systems and is found to be reasonable through numerical simulations.[5–8] In this approach

0146-9592/01/151131-03$15.00/0

$$A = a\exp[i\phi - iW(t-T) - (1+iC)(t-T)^2/2\tau^2], \tag{4}$$

where the amplitude a, phase ϕ, frequency W, time delay T, chirp C, and width τ all are functions of z. Each amplifier changes these parameters randomly by a small amount. If we denote changes in T and W by δT and δW, their variances and cross correlation can be obtained by substitution of Eq. (4) into the general formulas derived in Ref. 3. After some algebra, we obtain

$$\langle \delta T^2 \rangle = \frac{2S}{E^2}\int_{-\infty}^{\infty}(t-T)^2|B|^2 \mathrm{d}t = \frac{S\tau^2}{E}, \tag{5}$$

$$\langle \delta W^2 \rangle = \frac{2S}{E^2}\int_{-\infty}^{\infty}|B_t|^2 \mathrm{d}t = \frac{S(1+C^2)}{E\tau^2}, \tag{6}$$

$$\langle \delta T\, \delta W \rangle = \frac{iS}{2E^2}\int_{-\infty}^{\infty}(t-T)(B^*B_t - BB_t^*)\mathrm{d}t = \frac{SC}{E}, \tag{7}$$

where $B = A\exp(iWt)$, $S = n_{\mathrm{sp}}h\nu(G-1)$, n_{sp} is the population-inversion factor, $h\nu$ is the photon energy, and G is the gain of each amplifier.

We can use Eqs. (5)–(7) in combination with Eqs. (3) to calculate the total timing jitter σ_t. A relatively simple expression for σ_t is obtained when we consider the jitter at the end of last amplifier. For a periodic DM system with N amplifiers, we obtain

$$\begin{aligned}\sigma_t^2 &= \langle T^2\rangle - \langle T\rangle^2 \\ &= (S/E)\tau_0^2[N(1+C^2) + N(N-1)Cd \\ &\quad + \frac{1}{6}N(N-1)(2N-1)d^2],\end{aligned} \tag{8}$$

where τ, C, and E represent the width, chirp, and energy, respectively, of input pulses launched into the DM system. Note that $\tau = \tau_0(1+C^2)^{1/2}$, where τ_0 is the width of the unchirped pulse (at the transmitter). Details of the dispersion map enter into Eq. (8) through a single parameter, $d = \tau_0^{-2}\int_0^{L_A}\beta_2(z)\mathrm{d}z = \overline{\beta}_2 L_A/\tau_0^2$, where L_A is amplifier spacing and $\overline{\beta}_2$ is the average GVD over L_A. Equation (8) is valid even when L_A is a multiple of the map period (dense dispersion management).

In the case of DM solitons, we find input pulse parameters by use of the variational equations[5–8] and use Eq. (8) to calculate timing jitter. In practice, postcompensation can be used to reduce jitter. We have calculated the jitter at the end of the postcompensating fiber, using Eqs. (3). The result is

$$\sigma_c^2 = \sigma_t^2 + (S/E)\tau_0^2\{2NCd_c + Nd_c[(N-1)d + d_c]\}, \tag{9}$$

where $d_c = \beta_2 L_c/\tau_0^2$ is the dispersion length of the postcompensating fiber.

To study how postcompensation affects timing jitter, we consider a 40-Gbit/s soliton system with a dispersion map consisting of 10.5 km of anomalous-GVD fiber [$D = 4$ ps/(km nm)] and 9.7 km of normal-GVD fiber [$D = -4$ ps/(km nm)]. We choose $L_A = 4L_{\mathrm{map}}$ to ensure a realistic amplifier spacing of 80.8 km and use $\alpha = 0.2$ dB/km and $\gamma = 1.7\ \mathrm{W}^{-1}$/km as typical values of the fiber parameters. The input width $\tau = 6.87$ ps and chirp $C = 0.560$ are found by use of the periodicity conditions ($\tau_0 = 5.99$ ps). The soliton's peak power is 33 mW for periodic propagation and is used to find the pulse energy E. The spectral density S is calculated with $n_{\mathrm{sp}} = 1.3$ (noise figure, 4.1 dB). Figure 1 shows how σ_c varies with N for several values of $y = -d_c/(Nd)$, where y represents the fraction of postcompensation. Even a small value of postcompensation ($y = 0.25$) reduces jitter. Three most noteworthy features are that (i) jitter cannot be eliminated through postcompensation, (ii) jitter can be minimized with an optimum length of postcompensation fiber, and (iii) 100% postcompensation makes the situation worse compared with no compensation.

To estimate the maximum jitter reduction possible with postcompensation, we note that, for a long-haul system ($N \gg 1$), the N^3 term dominates in Eq. (8). The dominant terms in Eq. (9) are found to vary with y as

$$\sigma_c^2 \approx (S/E)\tau_0^2 N^3 \mathrm{d}^2\left(\frac{1}{3} - y + y^2\right). \tag{10}$$

The minimum value occurs for $y = 0.5$, and the jitter variance is reduced by a factor of 4 for this minimum value. The same conclusion was reached in an earlier study of constant-dispersion fibers.[9] Even though the N^3d^2 dependence of jitter is well known from previous work on constant-dispersion fibers, our approach is unique, as it provides simple analytic expressions for DM systems with arbitrary maps. It can also

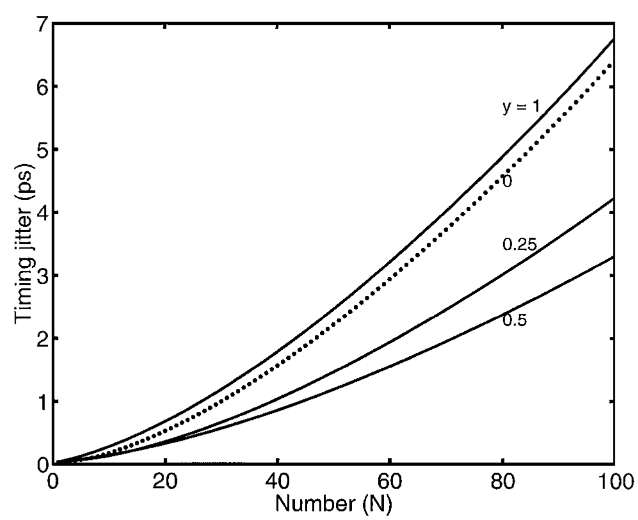

Fig. 1. Effect of postcompensation on the timing jitter of a 40-Gbit/s DM-soliton system for the dispersion map described in the text (four map periods over 80.8 km of amplifier spacing). Jitter, σ_c, is plotted as a function of the number of amplifiers for four values of y (the fraction of postcompensation).

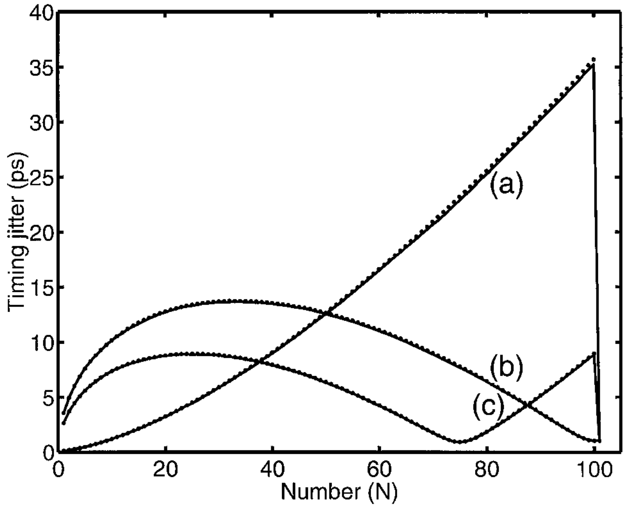

Fig. 2. Effect of precompensation and postcompensation on timing jitter of a 40-Gbit/s low-power (2.5-mW peak power) CRZ system for the dispersion map used in Fig. 1. (a) No precompensation and complete postcompensation, (b) complete precompensation and no postcompensation, (c) 75% precompensation and 25% postcompensation. The dots represent the results of numerical simulations.

be extended to the case of multiple amplifiers per map period.

We now consider a low-power CRZ system designed with precompensation and postcompensation fibers. Pulse evolution is not periodic in this case, but the dependence of the chirp and width on distance can be calculated analytically for a linear system.[2] Using the method described above, we obtain, the following simple analytic expression for the timing jitter:

$$\sigma_c^2 = (S/E)\tau_0^2[N + N(Nd + d_p + d_c)^2], \qquad (11)$$

where $d_p = \beta_{2p}L_p/\tau_0^2$ is the dispersion length of the precompensation fiber used to chirp the CRZ pulse before it enters the DM system. As before, the dominant term varies as N^3 when the average dispersion of the map is not zero. However, the jitter increases only linearly with N when $Nd + d_p + d_c = 0$, a condition that corresponds to zero net dispersion over the entire link.

One may ask if there is an optimum choice of d_p and d_c that would optimize such a CRZ system. To answer this question, in Fig. 2 we plot σ_c as a function of N, using Eq. (11) and the same dispersion map that was used in Fig. 1. The solid curves represent the analytical solution of Eqs. (3), and the dots represent their numerical solution averaged over 10^4 realizations. Figure 2 shows that our analytical predictions are consistent with numerical solutions of the moment equations on which they are based. More importantly, it shows that a specific choice of precompensation and postcompensation can minimize the jitter along the CRZ system. This may be desirable in practice to minimize pulse-to-pulse interactions. Curve (C) in Fig. 2 represents the optimum situation and corresponds to the choice $d_p \approx 3d_c$. We should stress that Fig. 2 shows jitter only at the amplifier locations. Jitter variation between two amplifiers should also be considered for a complete optimization.

In conclusion, we have presented an analytic theory of timing jitter in DM light-wave systems based on the moment method and the assumption of a chirped Gaussian pulse. We have applied it to a soliton system and found that postcompensation of the total accumulated dispersion by 50% can reduce the jitter by a factor of 2. We also applied our analytic theory to a low-power CRZ system and found that the jitter can be minimized all along the fiber link for an optimum choice of precompensation and postcompensation fibers. A comparison of DM versus CRZ systems shows that jitter is larger for CRZ systems when $d \neq 0$ because of lower pulse energies. Jitter becomes smaller when a CRZ system is designed with zero net dispersion, but this conclusion holds only for a truly linear system.

This research was supported in part by Corning, Inc., and the National Science Foundation. G. P. Agrawal's e-mail address is gpa@optics.rochester.edu.

References

1. J. P. Gordon and H. A. Haus, Opt. Lett. **11,** 665 (1986).
2. G. P. Agrawal, *Applications of Nonlinear Fiber Optics* (Academic, San Diego, Calif., 2001).
3. V. S. Grigoryan, C. R. Menyuk, and R. M. Mu, J. Lightwave Technol. **17,** 1347 (1999).
4. S. N. Vlasov, V. A. Petrishchev, and V. I. Talanov, Radiophys. Quantum Electron. **14,** 1353 (1971).
5. I. R. Gabitov, E. G. Shapiro, and S. K. Turitsyn, Opt. Commun. **134,** 317 (1997).
6. V. S. Grigoryan and C. R. Menyuk, Opt. Lett. **23,** 609 (1998).
7. A. Berntson, N. J. Doran, W. Forysiak, and J. H. B. Nijhof, Opt. Lett. **23,** 900 (1998).
8. T. I. Lakoba, J. Yang, D. J. Kaup, and B. A. Malomed, Opt. Commun. **149,** 366 (1998).
9. W. Forysiak, K. J. Blow, and N. J. Doran, Electron. Lett. **29,** 1225 (1993).